

PCCP

Accepted Manuscript



This is an *Accepted Manuscript*, which has been through the Royal Society of Chemistry peer review process and has been accepted for publication.

Accepted Manuscripts are published online shortly after acceptance, before technical editing, formatting and proof reading. Using this free service, authors can make their results available to the community, in citable form, before we publish the edited article. We will replace this *Accepted Manuscript* with the edited and formatted *Advance Article* as soon as it is available.

You can find more information about *Accepted Manuscripts* in the [Information for Authors](#).

Please note that technical editing may introduce minor changes to the text and/or graphics, which may alter content. The journal's standard [Terms & Conditions](#) and the [Ethical guidelines](#) still apply. In no event shall the Royal Society of Chemistry be held responsible for any errors or omissions in this *Accepted Manuscript* or any consequences arising from the use of any information it contains.

Controlling Charge Injection Properties in Polymer Field-Effect Transistor by Incorporation of Solution Processed Molybdenum Trioxide

Dang Xuan Long², Yong Xu², Huai-xin Wei², Chuan Liu^{1,3}, Yong-Young Noh^{2,*}*

¹ State Key Laboratory of Optoelectronic Materials and Technologies, Guangdong Province Key Laboratory of Display Material and Technology and School of Physics and Engineering, Sun Yat-sen University, Guangzhou 510275, People's Republic of China

² Department of Energy and Materials Engineering, Dongguk University, 26 Pil-dong, 3 ga, Jung-gu, Seoul 100-715, Republic of Korea

³ SYSU-CMU, Shunde International Joint Research Institute, Shunde, People's Republic of China

*Authors to whom corresponding should be addressed: electrical mail: liuchuan5@syzu.edu.cn, yynoh@dongguk.edu

Keywords: Organic Field-Effect Transistor, Charge injection, MoO₃, Contact Resistance, Conjugated Polymers

Abstract

A simply and facilely synthesized MoO₃ solution was developed to fabricate charge injection layers for improving the charge-injection properties in *p*-type organic field-effect transistors (OFETs). By dissolving MoO₃ powder in ammonium (NH₃) solvent under air atmosphere, an intermediate ammonium molybdate ((NH₄)₂MoO₄) precursor is made stable, transparent and to be spin-coated to form the MoO₃ interfacial layers, of which the thickness and morphology can be well-controlled. When the MoO₃ layer was applied to OFETs with a cost-effective molybdenum (Mo) electrode, the field-effect mobility (μ_{FET}) was significantly improved to be 0.17 or 1.85 cm²/V·s for polymer semiconductors, regioregular poly(3-hexylthiophene) (P3HT)

or 3,6-Bis-(5bromo-thiophen-2-yl)-*N,N'*-bis(2-octyl-1-dodecyl)-1,4-dioxo-pyrrolo[3,4-*c*]pyrrole (DPPT-TT), respectively. Device analysis indicate the MoO₃-deposited Mo contact exhibits contact resistance R_c of 1.2 M Ω ·cm comparable to that in device with the noble Au electrode. Kelvin-probe measurements show that the work function of the Mo electrode did not exhibit a dependence on the thickness of MoO₃ film. Instead, ultraviolet photoemission spectroscopy results show that a doping effect is probably induced by casting the MoO₃ layer on the P3HT semiconductor, which leads to the improved hole injection.

1. Introduction

Controlling the electrical properties of an interface is crucial for improving the characteristics of various organic devices.^{1, 2} The formation of benign contact properties for efficient charge injection from the metal electrode to organic semiconductors (OSCs) is the subject of much interest in organic field-effect transistors (OFETs)^{1, 3} because overall performance strongly depends on the charge-injection properties mainly characterized by contact resistance (R_c).^{4, 5} In particular, R_c in OFETs becomes dominant when the channel length decreases to less than 10 μm , which is a commercially meaningful dimension.⁶ On the one hand, in the laboratory Au has been commonly used as basic electrode in order to obtain low R_c for p -type OFETs because of its relatively deep work function ($W_f = 4.7 \sim 5.1$ eV) that is close to the highest occupied molecular orbital (HOMO) levels of typical p -type OSCs. On the other hand, the high price of Au ($\sim 50,000$ \$/kg) strongly limits its industrial applications and is unsuitable for low-cost electronics using printable OFETs.⁷ To reduce the material cost, the inexpensive element molybdenum (Mo) has been considered a very promising alternative because of a good electrical conductivity ($\sim 5.34 \times 10^6$ S/cm) and a reasonable price (~ 26 \$/kg). However, the relatively low W_f of as-deposited Mo electrode (4.3 \sim 4.6 eV) induces a significant obstacle for hole injection to the commonly used p -type OSCs (HOMO = $-4.5 \sim -5.8$ eV).^{2, 8} Therefore, an efficient hole injection layer (HIL) is needed to modify Mo electrodes by either tuning the W_f or inducing dopants *via* charge transfer.

For this purpose, one of the most promising candidates is molybdenum oxide (MoO_3), which has deep-lying electronic states and is non-toxic.⁹ In particular, MoO_3 can be solution-processed to allow low-cost and large-area fabrication by cost-effective printing processes. Several methods to make precursors for fabricating a solution-processed MoO_3 layer have been reported.^[10–14] Qiu et al. spin-coated an ammonium heptamolybdate $(\text{NH}_4)_6\text{Mo}_7\text{O}_{24} \cdot \text{H}_2\text{O}$ precursor solution on indium tin oxide (ITO) and treated at 160 $^\circ\text{C}$ in order to obtain a MoO_3 nanoparticles film.¹⁰ In addition, the Yang group was pre-heating the same precursor in deionized water before spin coating and obtained a smooth MoO_3 film.¹¹ The sol-gel technique of dissolving MoO_3 powder in H_2O_2 can provide a $\text{MoO}_2(\text{OH})(\text{OOH})$ precursor, but it requires a very high annealing

temperature (275 °C) for the conversion of the precursor to MoO₃.¹² Similarly, a MoO₃ solution by dispersing molybdenum powder in ethanol and H₂O₂ mixed solvents was developed, but a long reaction time (18 h) was needed.¹³ In general, toward scalable and reliable fabrications, an ideal solution-processed technique of MoO₃ should be featured with a low processing temperature, a short reaction time, simple and low-cost processing steps, low surface roughness of the deposited film, and a feasible way to control device parameters such as contact resistance. However, most recent work has focused on improving charge injection properties in organic photovoltaic cells and a report has also been published for improving OFETs through the interlayer.

Here we report a method to improve the charge-injection properties in OFETs with cost-effective Mo electrodes using a solution-processable MoO₃ interlayer. It was necessary that we develop a highly concentrated MoO₃ aqueous solution, which is achieved by synthesis of an ammonium molybdate ((NH₄)₂MoO₄) precursor via reaction with MoO₃ powder, H₂O, and NH₃. The solution was spin-coated and moderately annealed to form the MoO₃ interfacial layer between the source/drain electrode and a *p*-type polymer semiconductor layer, which was made of regioregular poly(3-hexylthiophene) (P3HT) or 3,6-Bis-(5bromo-thiophen-2-yl)-*N,N'*-bis(2-octyl-1-dodecyl)-1,4-dioxo-pyrrolo[3,4-*c*]pyrrole (DPPT-TT). The MoO₃ interlayer significantly improved the μ_{FET} of the Mo contacted OFETs up to values that are comparable to those of devices with a pristine Au electrode. Device analysis showed that the MoO₃ deposited Mo electrode exhibits reduced R_c values that are one sixth of that of devices with bare Mo contacts. The combined, systematic study using Kelvin probe and ultraviolet photoemission spectroscopy (UPS) reveal that, the improved contact properties are mainly attributed to doping of OSCs at the metal–semiconductor interface by the MoO₃ interfacial layer rather than a work-function change of Mo.

2. Experimental

Interlayer processing: The process for fabricating the MoO₃ solution is displayed in **Fig. 1(a)**. The MoO₃ solution was synthesized by dissolving MoO₃ powder in ammonium (NH₃) solvent under air atmosphere. The flask was opened during the synthesis process to supply enough water vapor from the ambient atmosphere. The solution was heated at 80°C for 1 h with stirring in air

and the color of solution changed to transparent ammonium molybdate ((NH₄)₂MoO₄) solution. At a lower temperature (60°C) MoO₃ did not dissolve well at high concentration, while at a higher temperature (120°C) NH₃ started evaporating as vapor out from solution and (NH₄)₂MoO₄ easily decomposed. The heating time of 1 hour is necessary to completely dissolve MoO₃. The aqueous transparent solution with MoO₃ in ammonia–water is formed by the chemical reaction between MoO₃, H₂O, and NH₃ as follows,



The desired concentration was achieved by diluting a saturated solution (~20 mg ml⁻¹) into a certain amount of deionized water. The ammonium molybdate (NH₄)₂MoO₄ is soluble in H₂O and the solution is transparent, colorless, and fairly stable without any change in color or transmittance in ambient conditions for 2 months. The resulting solution was diluted by deionized water to various concentrations (0.2 ~ 1.6 wt%) and was used to form the MoO₃ films. The aqueous MoO₃ solution was spin-coated onto a pristine Mo surface and annealed at 150 °C for 10 min in air. This temperature is for the chemical decomposition from ammonium molybdate to molybdenum oxide and to remove all the remaining NH₃ in the film. During the annealing process, the ammonium molybdate underwent rapid decomposition to three components: MoO₃, NH₃, and H₂O, among which NH₃ and H₂O was evaporated into the air and MoO₃ was left in the film. Prolonged heating promotes the growth of MoO₃ crystals, which are no longer soluble in the aqueous solution.¹⁴ Apparently, the preparation of the MoO₃ solution described here is very simple and cost-effective, employing a cheap and commercially available precursor, an environmentally friendly solvent of deionized water, and a low-temperature process under ambient conditions.

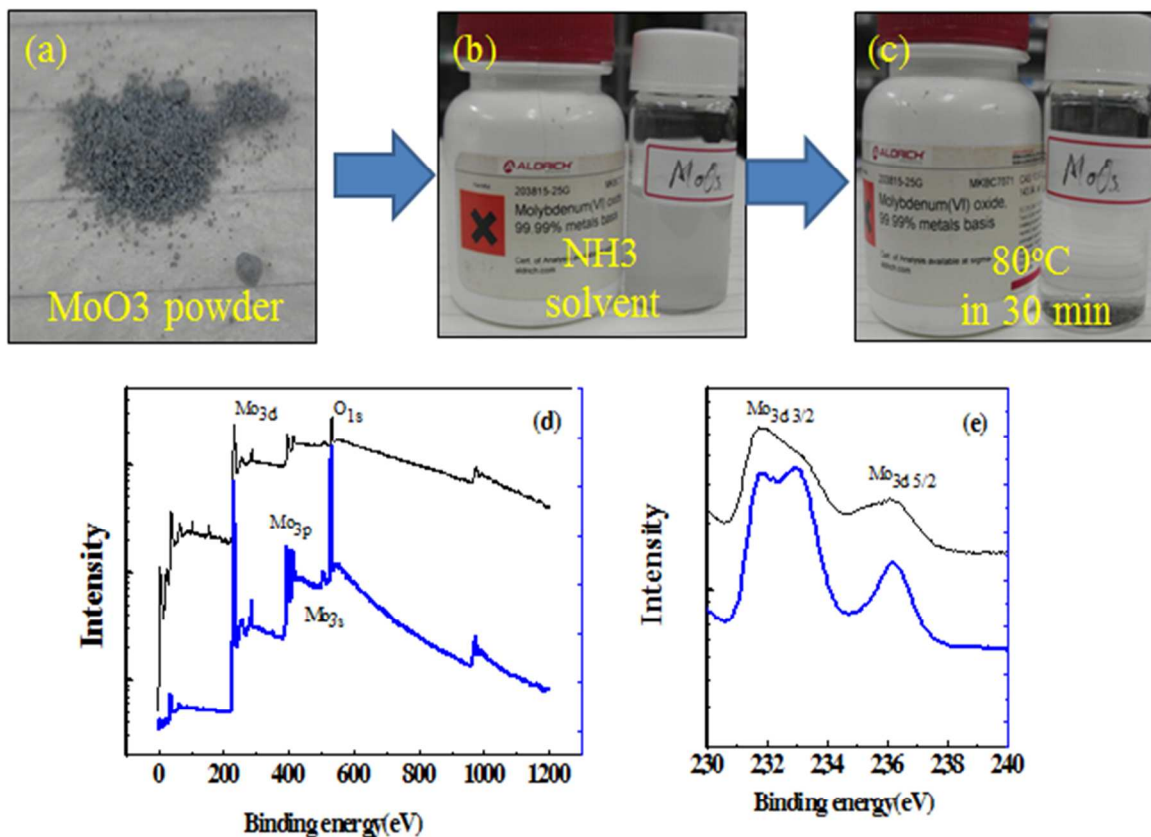


Figure 1 (a–c) Digital camera images of MoO₃ powder, solution in NH₃ solvent, and after heating at 80 °C for 30 min. X-ray photoemission spectra of the MoO₃ films: (d) full scanned spectra, (e) Mo 3d core level of solution-processed MoO₃. The black and blue curves denotes the signals of the film prepared from 2 and 8 mg/ml solutions, respectively.

Film Characterization: The surface morphology of the thin film was investigated using a tapping-mode atomic force microscope (AFM) (Nanoscope III, Veeco Instruments, Inc.) at the Korea Basic Science Institute (KBSI). X-ray photoemission spectroscopy (XPS) and UPS were measured using AXIS-NOVA (Kratos, Inc.) with a base pressure of 4.2×10^{-9} Torr. A Kelvin probe (KP 6500 Digital Kelvin probe, McAllister Technical Services, Co. Ltd) was used to measure the W_f of the contact metal and the contact interlayer.

Field-effect transistor fabrication and characterizations: OFETs with a top-gate/bottom-contact (TG/BC) structure were fabricated on glass substrates. After the conventional photolithography process of developing photoresist in order to pattern the source/drain electrodes, a ~3 nm-thick Ni adhesion layer and ~13 nm-thick Mo layer were deposited by sputtering the Mo target on the Corning Eagle 2000 glass substrates, followed by a lift-off process. The source/drain electrodes define various channel lengths (L) of 2, 5, 10, or 20 μm with a uniform channel width (W) of 1 mm. The Mo/Ni-electrode patterned substrates were cleaned sequentially in an ultrasonic bath with de-ionized water, acetone, and iso-propanol for 5 min for each. A MoO_3 interlayer solution with different concentrations (0.2–0.8 wt%) was spin-coated on a pre-cleaned substrate and then annealed at 150 $^\circ\text{C}$ for 20 min. A p -type polymer semiconductor, P3HT, was purchased from Sigma-Aldrich and DPPT-TT was chemically synthesized using a previously published procedure and dissolved in anhydrous dichlorobenzene (DCB) in order to obtain a ~10 mg/ml concentration solution. The solution was spin-coated onto the MoO_3 interlayer-deposited substrates and sequentially annealed at 150 $^\circ\text{C}$ (for P3HT) or 300 $^\circ\text{C}$ (for DPPT-TT) for ~30 min in a nitrogen (N_2)-filled glove box. A polymer dielectric layer of poly(methyl methacrylate) (PMMA) was purchased from Sigma-Aldrich, used without further purification, and dissolved in n -butylacetate (nBA) at 80 mg/ml concentration. The PMMA thin film was formed on the p -type polymer semiconductor layer by spin-coating followed by thermal annealing at 80 $^\circ\text{C}$ for ~30 min in the same N_2 -filled glove box in order to remove the residual solvents. The OFET fabrication was completed by thermally depositing aluminum (Al) *via* metal shadow masks in order to form top-gate electrodes (~50 nm thick). The OFETs' electrical characteristics were tested by using a Keithley 4200 semiconductor characterization system in the N_2 -filled glove box. The corresponding field-effect mobility (μ_{FET}) and threshold voltage (V_{Th}) were calculated from the saturation regime (at a drain voltage $V_d = -100\text{V}$). The low-field mobility (μ_0) and R_C were evaluated by the Y-function method (YFM)^{4, 15} for individual transistors.

Estimation of depletion width at the contact. We present how to calculate W_d in 3 steps as below. First, according to the semiconductor physics, the intrinsic carrier concentration is calculated by,

$$n_i = (N_C N_V)^{0.5} \exp(-E_g/2kT) \quad (1)$$

Here N_C and N_V are the density of states in conduction band and valence band, respectively, k is

the Boltzmann constant, T is the temperature, and E_g is the band gap of the polymeric semiconductor. Second, with the calculated n_i , the hole concentration N_a is calculated by,

$$N_a = n_i \exp[(E_{fi} - E_f)/kT] \quad (2)$$

Here E_{fi} is the intrinsic Fermi level and E_f is the Fermi level of semiconductor after doping.

Third, with the calculated N_a , the depletion width W_d is calculated by,

$$W_d = [2\varepsilon_{SC}V_{bi}/qN_a]^{0.5} \quad (3)$$

Here ε_{SC} is the dielectric constant of semiconductor, q is the electron charge, and V_{bi} is the built-in potential that is the difference between E_f and the work-function of contact electrode (Φ_m), i.e. $V_{bi}=E_f-\Phi_m$ (for hole injection). Determining the exact value of depletion width (W_d) needs accurate measurement of Fermi-level. For roughly estimating W_d of P3HT/MoO₃/Mo OFETs, the constants and parameters of materials are list in the supporting information.

3. Results and Discussion.

The component and the surface electronic structure of the solution-processed MoO₃ film was investigated by X-ray photoemission spectroscopy (XPS). In **Fig. 1(b)**, the peaks of the core levels of N are not found for the MoO₃ film, suggesting that the synthetic precursor containing the N completely decomposes to MoO₃ by annealing at the temperature of 150 °C. In agreement with previous reported results in the literature, all the core levels of Mo can be seen clearly in the full spectrum of solution-processed MoO₃ film except for other small peaks due to sample contamination. The spectra were identical for both films with different concentration without any shift, indicating that uniform and conductive MoOx films are on the substrate. The characteristic peaks of the O1s, Mo3s, Mo3p and Mo3d levels of the MoO₃ film are identical for both concentrations. As the solution concentration increased from 2 mg/ml to 8 mg/ml, a higher peak density of Mo3d and O1s was found, indicating a larger amount of MoO₃ on the Mo substrate. **Figure 1(c)** shows the core level of Mo3d with the Mo3d5/2 and Mo3/2 peaks located at 236.3 eV and 233.2 eV, respectively, which indicates the presence of the Mo6+ cation as the characteristic peak of molybdenum.

The thickness and quality, i.e., roughness and uniformity, of the deposited MoO₃ films are determined by a variety of experimental factors including the viscosity and surface tension of the solvent, solid contents of the coating solution, surface energy of the substrate, distance between

the spray nozzle and substrate, and spin-coating speed. **Figure. 2** shows AFM images of the MoO₃ films coated from solution with different concentrations: 2, 4, and 8 mg/ml. The deposition of MoO₃ on the glass substrate from a 2-mg/ml solution resulted in discrete nanoplates, which are formed by the aggregation of MoO₃ nanoparticles. However, the same deposition on the Mo substrates generated nanoplates (made of sub-micrometer size crystallites) without observable aggregation and the roughness of MoO₃ film is small ($R_q \sim 0.44$ nm). By further increasing the concentration of MoO₃ in the ammonia–water, the density of the nanoplates increases and a continuous and smooth MoO₃ film was formed with slightly increased roughness (0.557 nm at 4 mg/ml and 0.750 nm at 8 mg/ml). Such a low roughness of the channel region would hardly affect the performance of our top-gate OFETs because the charge transport in top-gated OFETs mainly occurs on the upper surface of the semiconductor layer. Moreover, we observed that the MoO₃ layer made the Mo substrates more hydrophilic, which may alleviate dewetting or delaminating of organic films on the electrodes.

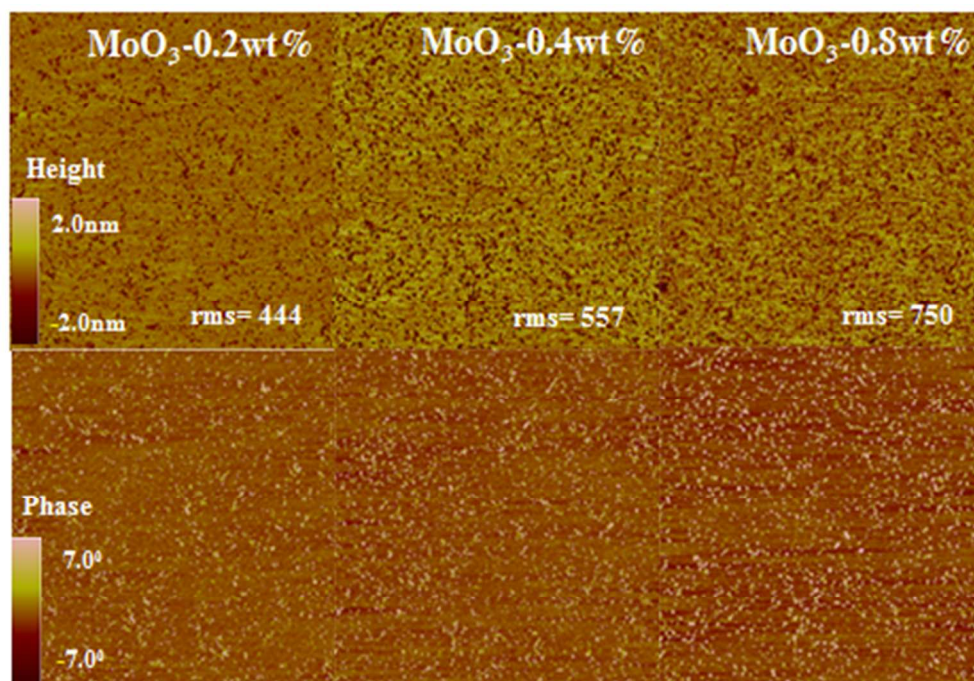


Figure 2 AFM images of MoO₃ films when spin coated by MoO₃ solution at concentration 0.2–0.8 wt% on Mo substrate (the units of rms are 0.001 nm).

The OFETs configuration and molecular structures of the semiconducting polymers P3HT and DPPT-TT are shown in **Fig. 3**. The measured transfer and output characteristics are shown in **Fig. 4**, including the devices with pristine Mo electrodes and MoO₃-deposited Mo electrodes. The key parameters, such as the μ_{FET} in the saturation regime (at $V_d = -100\text{V}$), V_{Th} , on/off-current ratio ($I_{\text{on}}/I_{\text{off}}$), and subthreshold swing (SS), are listed in **Table 1**. The P3HT OFETs with pristine Au electrodes are found to have a reasonably high hole μ_{FET} of $\sim 0.15 \text{ cm}^2\text{V}^{-1}\text{s}^{-1}$ and moreover no significant nonlinearity was observed in the output characteristics at small drain voltage (V_d), indicative of nearly Ohmic contacts. Compared to Au, bare Mo contacts lead to severe super-linear curves in the linear region of the output characteristics, large hysteresis, very small output current, and a reduced hole mobility ($0.08 \text{ cm}^2\text{V}^{-1}\text{s}^{-1}$), as shown in **Fig. 4 (a)**. Apparently because of the large barrier to hole injection from Mo into P3HT (0.62 eV), R_C is supposed to become significant and to limit the hole transport in the channel. In contrast, by adding a thin interlayer of MoO₃ between the Mo and P3HT, the interfacial injection is substantially enhanced and the overall performance is improved, manifested by a high output current, absence of hysteresis, and a higher mobility of $0.17 \text{ cm}^2\text{V}^{-1}\text{s}^{-1}$ as comparable to the OFETs with Au contacts (see **Fig. 4**). For a reference, the performance of OFETs with MoO₃/Au contacts are shown in supporting information **Fig. S1**. Similarly, the DPPT-TT OFETs also showed a notably improved hole mobility ($1.85 \text{ cm}^2\text{V}^{-1}\text{s}^{-1}$) after inserting the MoO₃ interlayer to Mo source/drain electrodes with respect to counterparts that only incorporate pristine Mo contacts ($1.20 \text{ cm}^2\text{V}^{-1}\text{s}^{-1}$) (Supporting information **Fig. S2**).

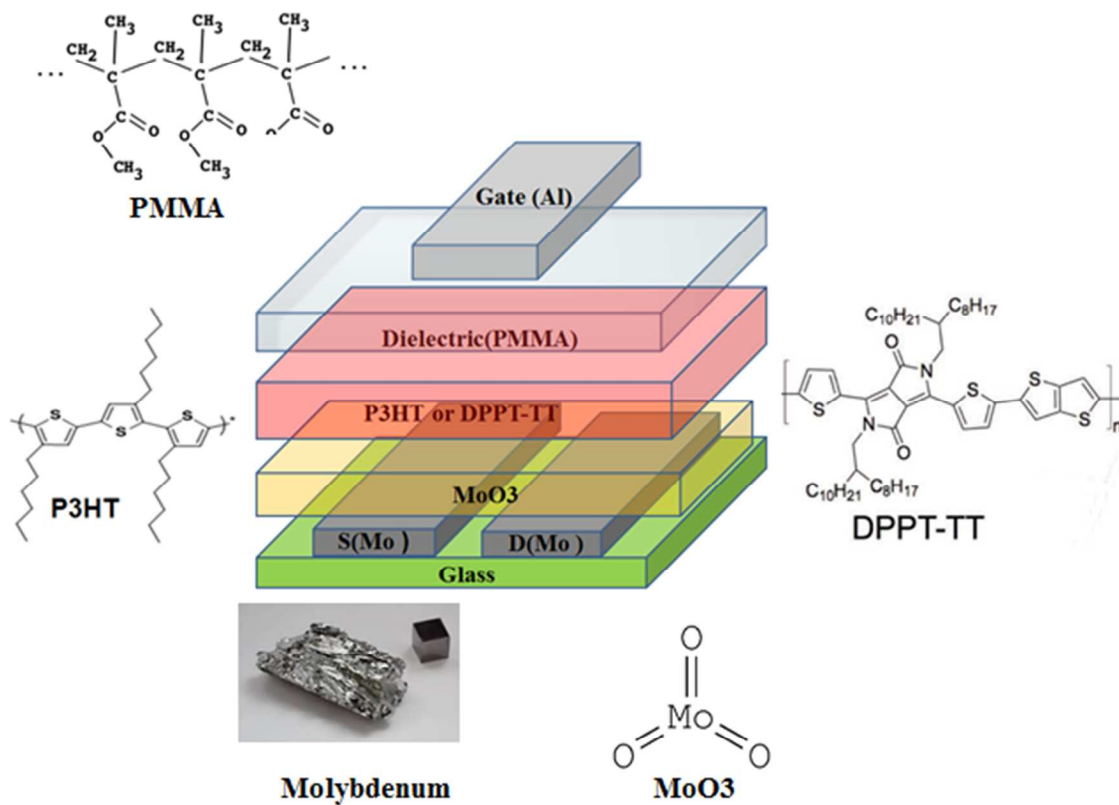


Figure 3 Molecular structures of P3HT, DPPT-TT, MoO₃, and PMMA and digital camera images of Molybdenum. Structure of a top-gate/bottom-contact OFET device with MoO₃ interlayer on Mo source/drain electrode.

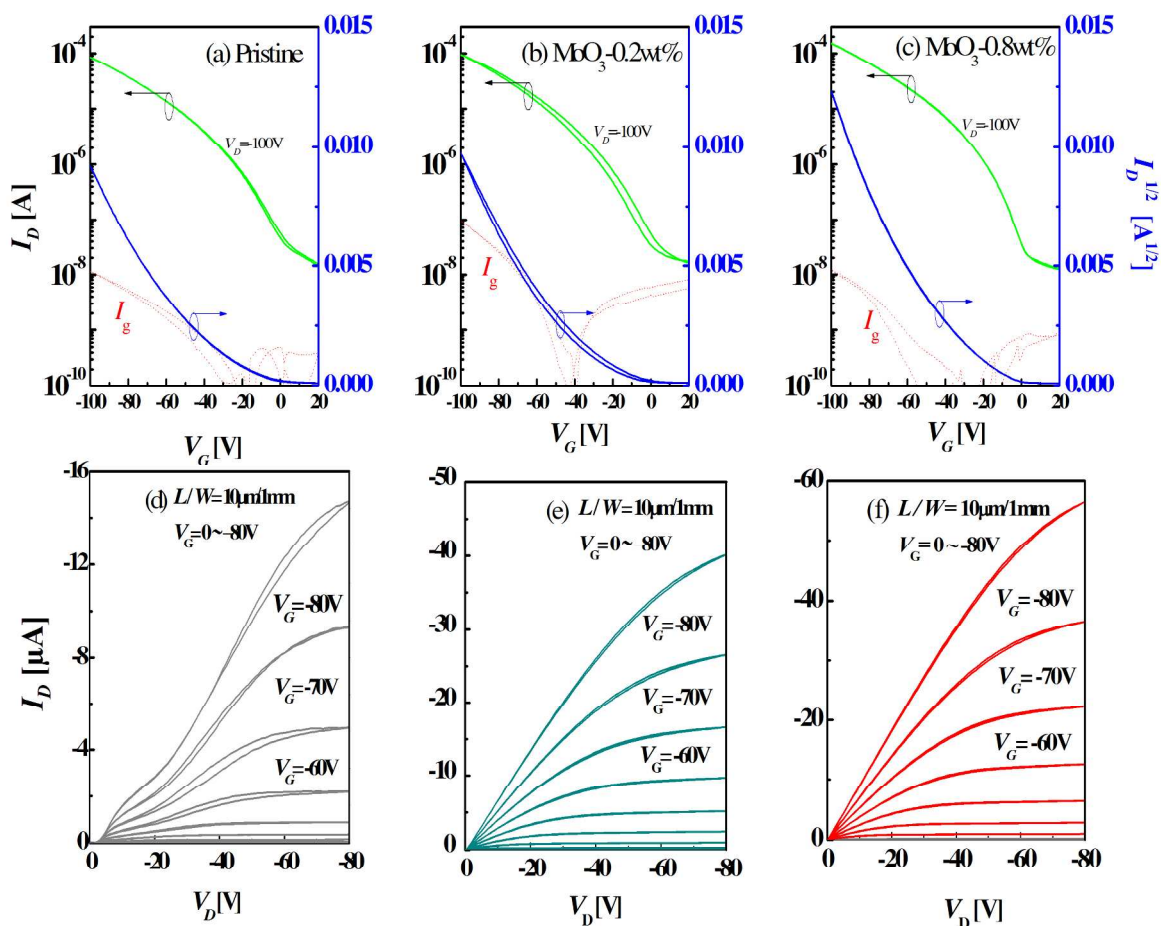


Figure 4 Transfer (I_d vs. V_g) and output (I_d vs. V_d) characteristics of the OFETs with *p*-type polymer semiconductors, P3HT and Mo electrodes with and without MoO₃ interlayer (0.2–0.8 wt%); (a,d) P3HT OFETs with pristine Mo source/drain electrodes, (b,e–c,f) P3HT OFETs with MoO₃-deposited Mo electrodes.

Table 1. Fundamental device parameters of the P3HT and DPPT-TT OFETs with Mo metal electrodes: pristine Mo and MoO₃-deposited Mo electrodes. The field-effect mobility (μ_{FET}) and V_{Th} are obtained from the gradual channel approximation at the saturation region (at $V_{\text{d}} = -100\text{V}$), $W/L = 1.0 \text{ mm}/20 \mu\text{m}$, and dielectric capacitance per unit area (C_i) is $\sim 6.2 \text{ nF/cm}^2$.

OSC	Concentration of MoO ₃ interlayer (wt%)	Annealing temperature/time (°C/min)	μ_{h} [cm^2/Vs]	$V_{\text{Th,h}}$ [V]	$I_{\text{On/off}}$
P3HT	None	150/30	0.08 (± 0.01)	-30.2 (± 2.17)	10^3
	0.2	150/30	0.12 (± 0.006)	-32.8 (± 2.67)	10^3
	0.4	150/30	0.14 (± 0.008)	-30.6 (± 3.54)	10^3
	0.8	150/30	0.17 (± 0.01)	-28.7 (± 2.15)	10^3
	1.6	150/30	0.1 (± 0.01)	-25.7 (± 2.53)	10^3
	Au electrode	150/30	0.15 (± 0.01)	-31.8 (± 3.33)	10^3
DPPT-TT	None	300/30	1.2 (± 0.01)	-65.2 (± 2.17)	10^3
	0.2	300/30	1.35 (± 0.006)	-62.8 (± 2.67)	10^3
	0.4	300/30	1.57 (± 0.008)	-60.6 (± 3.54)	10^3
	0.8	300/30	1.85 (± 0.01)	-58.7 (± 2.15)	10^3

Au electrode	300/30	1.9 (± 0.02)	-63.5 (± 3.21)	10^3
--------------	--------	-----------------------	-------------------------	--------

We henceforth probe the mechanism of controllable, enhanced hole injection with the solution-processed MoO₃ layers. We begin from the energy levels related to the charge injections as shown in **Fig. 5(a)**, which illustrate the mismatched energy levels for hole injection between the semiconductor's HOMO levels and the W_f of the Mo electrodes. In the case of Au, the barrier height (E_b) of ~ 0.2 eV for hole injection is not severe when compared with that of Mo, which has ~ 0.75 eV for P3HT OFETs. Therefore, this large charge-injection barrier (about 0.6 eV greater than Au) can lead to increased R_C , thereby degrading the performance of the OFETs by decreasing their apparent mobility. To check the W_f change upon adding MoO₃ layers, we employed the Kelvin probe to determine W_f . Though the W_f of pristine MoO₃ is -5.5 eV in theory, in our devices the W_f of the MoO₃-coated Mo electrodes ranges from -4.40 eV to -4.47 eV as the MoO₃ solution concentration increased from 0.1 to 0.8 wt% (**Fig. 5(b)**). Normally the W_f of the metal electrodes was supposed to be changed by the charge transfer between the interlayer (MoO₃ here) and the electrodes. For example, when applying the MoO₃ interlayer to the other electrode Ti ($W_f = 4.3$ eV), the W_f was gradually changed from 4.3 eV to 4.7 eV by changing the concentration of MoO₃, as shown in **Fig. S4**. However, in the case of MoO₃-deposited Mo electrodes, the W_f was pinned to be around the original value 4.45 eV, not depending on the thickness of the MoO₃ film. Based on the above observations, we propose that the bare Mo has been readily oxidized and covered by a thin layer of MoO₃ and that it contains the Mo-O-Mo3d(+5) or Mo-O-Mo3d(+6) complexes. As a result, the measured W_f by Kelvin probe for the electrode is around 4.40 eV rather than 5.5 eV of Mo. When depositing extra MoO₃ interlayers, as there is no charge transfer occurring, the measured W_f of the electrode is then pinned around 4.40 eV without changing with subsequent MoO₃ deposition. Hence, the improved hole-injection in OFETs by the deposited MoO₃ is not because of the change in work function of the bottom contact electrodes; rather, we propose that the improved hole-injection barrier by the deposited MoO₃ is not due to the change in work function of the bottom contact electrodes.

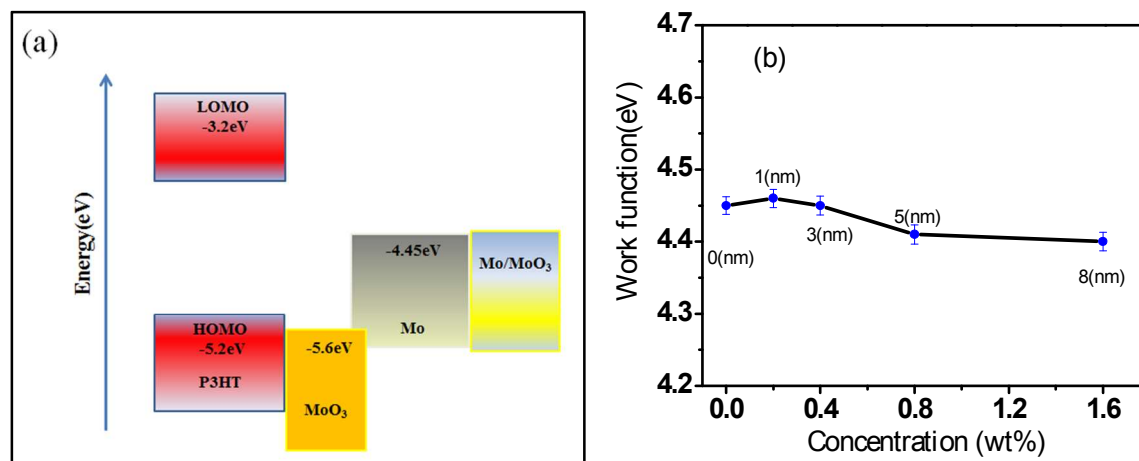


Fig. 5 (a) Energy level alignment of organic semiconductor on Mo S/D electrode. (b) Work function of Mo electrode dependence on MoO₃ thickness (for changing concentration of MoO₃ solution).

We employed UPS measurement in order to investigate the electronic structure of the MoO₃/P3HT interface. First, a bare sample of P3HT thin film (ca. 30 nm) was spin-coated on Mo deposited on a glass substrate (the pre-deposited Mo on glass is to provide a conducting surface for UPS measurement) and the top surface of P3HT semiconductor was exposed to ultraviolet (UV) irradiation for UPS measurement. For analysis of the MoO₃ and P3HT interface, MoO₃ was thermally deposited onto a P3HT film that was spin-coated on a Mo substrate. **Figure 6** shows the UPS spectra of a Mo-P3HT-MoO₃ film (from the bottom to the top). From the UPS spectra at the secondary-electron cut-off position, the binding energy of the polymer progressively decreased with thicker MoO₃ on the surface: 19.71 eV for P3HT, 19.42 eV at 1 nm of MoO₃ on P3HT, 18.58 eV at 2 nm, 18.93 eV at 3 nm, respectively. It corresponded to the increased W_f of the films.¹⁶ **Figure 6** also shows that the energy difference between the valence edge and the Fermi energy level (at zero binding energy) decreases from 1.5 eV for the pristine P3HT film to 0.46 eV in the film with 3 nm MoO₃. As this signal may come from the P3HT/MoO₃ interface and/or the MoO₃ layer, it probably indicates *p*-doping as the thickness of MoO₃ is increased.

Combining the observations from the Kelvin Probe and UPS studies, it can be postulated that the role of the MoO₃ interlayer is not for shifting the work function of the Mo electrode but

rather involves the doping of P3HT and perhaps providing gap states for tunneling. The overall enhanced injection by MoO₃ then comes from the interfacial and bulk effects. The interfacial effects include the narrowed depletion width at the interface¹⁷ and extra gap states provided by MoO₃, both of which enhance the tunneling probability. The bulk effect refers to the moderately doping of P3HT semiconductor, so that carrier concentration is increased, bulk conductivity closed to the contacts is enhanced, and bulk trap states are partially filled^{18, 19}. These synergistic effects explain the enhancement of *p*-channel injection and transport of P3HT OFETs. Though quantifying each effect is difficult, here we roughly estimate the effect of narrowing W_d (see experimental and supporting information for the methods). Originally, W_d is over 1 μm without MoO₃ doping and it becomes 5.4 nm and 0.8 nm if assuming that Fermi-level shift reaches 0.9 eV and 1.0 eV (corresponding to the signal detected by UPS when the MoO₃ layer is of 2 nm and 3 nm). That is, if with a large shift in Fermi level of 1eV, tunneling would be much enhanced.

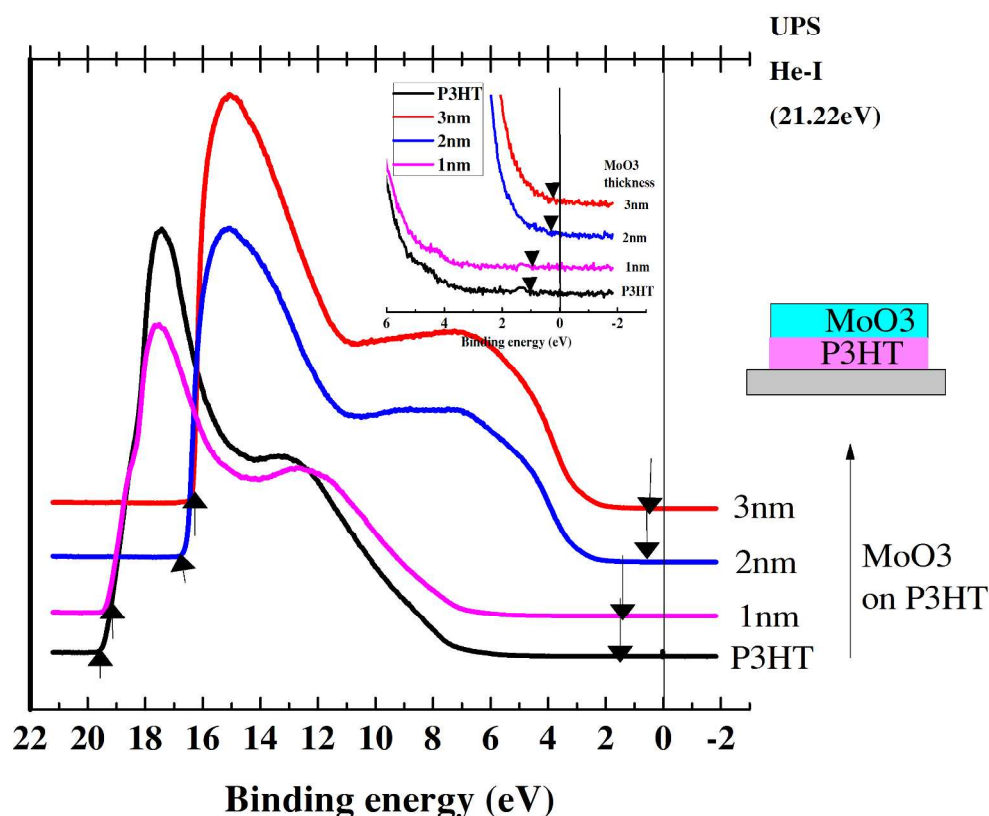


Fig 6. UPS spectra of different thermally deposited MoO₃ thicknesses on P3HT thin film.

To quantify the link between the interfacial electronic structures and the device injection parameter R_C , we used the YFM to evaluate the R_C for individual OFETs, which is considered a fast and precise method for obtaining R_C .^{15,20} **Figure 7** shows R_C for the P3HT OFETs with bare Mo and MoO₃ layer-deposited Mo electrodes (Mo/MoO₃) by solution process. One can readily find that compared to the case of pristine Mo, R_C is decreased by adding MoO₃ interlayer (even at a low concentration of 0.1 wt%) and the related R_C strongly depends on the MoO₃ concentration. This result suggests that the thin MoO₃ interlayer enhanced the hole injection/extraction so that the R_C is reduced from 6.1 M Ω to 1.1 M Ω as the thickness of MoO₃ increases from 1 nm to 5 nm (0.2 to 0.8 wt%). This is in good agreement with above hypothesis that a thin interlayer of MoO₃ promotes hole injection by moderately doping polymeric semiconductors and perhaps introduces interface states that provide charge-hopping gap states. For the thicker film of 8 nm, again R_C increased to 4.3 M Ω at 8 nm MoO₃ film (1.6 wt%). This is because the film shows higher defect density and surface roughness, probably inducing poorer surface roughness, high trap density of the film, and an elevated injection barrier by forming a metal–insulator–semiconductor structure at the contacts.

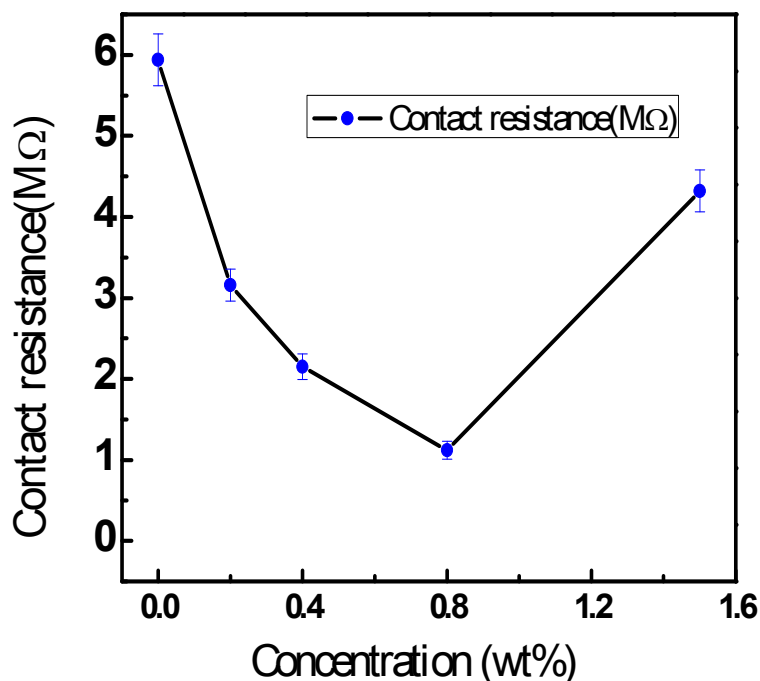


Fig 7. Contact resistance of the P3HT OFETs with pristine Mo or MoO₃-deposited Mo electrodes (Mo/MoO₃) when concentration of MoO₃ is varied from 0.2 to 1.6 wt%. The R_c is evaluated by the Y-function method (YFM) at low V_d of -0.5 or -1.0 V.

4. Conclusion

In conclusion, we demonstrated high-performance P3HT and DPPT-TT organic field-effect transistors utilizing a contact interlayer of MoO₃ made by a facile and cost-effective solution process. The MoO₃ solution is prepared by heating an aqueous solution of a precursor, MoO₃ powder in NH₃ solvent, at a moderate temperature of 80 °C for only 1 hour. The OFETs with the MoO₃-deposited Mo electrodes exhibited improved performance comparable to that with Au contacts. It is found that the interlayer hardly changed the work function of Mo but that the improved performance is related to the doping of the *p*-type polymer semiconductors and/or extra gap-states after the incorporation of the transition metal oxide interlayer of MoO₃. This technique should enable the development of large-area, low cost electronics with Mo electrodes and MoO₃ interlayers.

Acknowledgements:

The authors gratefully acknowledge the financial support of the project from National “985” Project (30000-31101200), “863” Program (2014AA033002; 2015AA033408), and the Economic and Information Industry Commission of Guangdong Province. The work is partially supported by Shunde Government, Guangdong Province, China, under the Contract No. 20140401. This work is also partially supported by the National Research Foundation of Korea (NRF) grant funded by the Korean Government (MSIP) (NRF-2014R1A2A2A01007159).

References

1. S. W. Rhee and D. J. Yun, *J. Mater. Chem.*, 2008, 18, 5437-5444.
2. D. Natali and M. Caironi, *Adv. Mater.*, 2012, 24, 1357-1387.
3. M. T. Greiner, L. Chai, M. G. Helander, W.-M. Tang and Z.-H. Lu, *Adv. Funct. Mater.*, 2013, 23, 215-226.
4. C. Diouf, A. Cros, S. Monfray, J. Mitard, J. Rosa, D. Gloria and G. Ghibaudo, *Solid-State Electron.*, 2013, 85, 12-14.
5. C. Liu, Y. Xu and Y.-Y. Noh, *Mater. Today*, 2015, 18, 79-96.
6. K. J. Baeg, J. Kim, D. Khim, M. Caironi, D. Y. Kim, I. K. You, J. R. Quinn, A. Facchetti and Y. Y. Noh, *Acs Applied Materials & Interfaces*, 2011, 3, 3205-3214.
7. D. X. Long, Y. Xu, S.-J. Kang, W.-T. Park, E.-Y. Choi, Y.-C. Nah, C. Liu and Y.-Y. Noh, *Organic Electronics*, 2015, 17, 66-76.
8. S. Braun, W. R. Salaneck and M. Fahlman, *Adv. Mater.*, 2009, 21, 1450-1472.
9. G. Wang, T. Jiu, P. Li, J. Li, C. Sun, F. Lu and J. Fang, *Sol. Energy Mater. Sol. Cells*, 2014, 120, 603-609.
10. W. Qiu, A. Hadipour, R. Muller, B. Conings, H.-G. Boyen, P. Heremans and L. Froyen, *Acs Applied Materials & Interfaces*, 2014, 6, 16335-16343.
11. S. Murase and Y. Yang, *Adv. Mater.*, 2012, 24, 2459-2462.
12. C. Girotto, E. Voroshazi, D. Cheyns, P. Heremans and B. P. Rand, *Acs Applied Materials & Interfaces*, 2011, 3, 3244-3247.
13. F. Xie, W. C. H. Choy, C. Wang, X. Li, S. Zhang and J. Hou, *Adv. Mater.*, 2013, 25, 2051-2055.

14. J. Liu, X. Wu, S. Chen, X. Shi, J. Wang, S. Huang, X. Guo and G. He, *Journal of Materials Chemistry C*, 2014, 2, 158-163.
15. Y. Xu, T. Minari, K. Tsukagoshi, J. A. Chroboczek and G. Ghibaudo, *J. Appl. Phys.*, 2010, 107, 7.
16. M. T. Greiner, L. Chai, M. G. Helander, W. M. Tang and Z. H. Lu, *Adv. Funct. Mater.*, 2012, 22, 4557-4568.
17. D. Khim, K.-J. Baeg, M. Caironi, C. Liu, Y. Xu, D.-Y. Kim and Y.-Y. Noh, *Adv. Funct. Mater.*, 2014, 24, 6252-6261.
18. T. Minari, P. Darmawan, C. Liu, Y. Li, Y. Xu and K. Tsukagoshi, *Appl. Phys. Lett.*, 2012, 100.
19. S. Hamwi, J. Meyer, T. Winkler, T. Riedl and W. Kowalsky, *Appl. Phys. Lett.*, 2009, 94.
20. Y. Xu, T. Minari, K. Tsukagoshi, R. Gwoziecki, R. Coppard, F. Balestra and G. Ghibaudo, *Organic Electronics*, 2011, 12, 2019-2024.